

# Dense Plasma Effects on Nuclear Reaction Rates

E. L. Pollock and B. Militzer  
*Physics Department,  
Lawrence Livermore National Laboratory,  
University of California, Livermore, California 94550*  
(Dated: November 14, 2003)

Plasma density effects can cause an exponential change in charged particle nuclear reaction rates important in stellar evolution. Reaction rates in dense plasma, with emphasis on quantum aspects, are examined here using path integral Monte Carlo. Quantum mechanics causes a reduction in the many body enhancement of the reaction rate compared to the value for a classical system. This can be attributed to the “quantum smearing” of the short range Coulomb interaction resulting in reduced repulsion between the reacting pair and surrounding particles. Electron screening and ion exchange effects are also examined, with screening reducing and exchange slightly increasing the many body enhancement.

*Introduction*– Information on nuclear reaction rates is commonly obtained from two particle scattering experiments. Applications however, particularly in key questions of stellar evolution and inertial confinement fusion, often involve many body environments where density effects can produce orders of magnitude changes in reaction rates. Quantum mechanics can markedly alter this many body enhancement. In this letter a systematic investigation of reaction rate enhancement due to density effects, including electron screening and ion exchange, based on path integral Monte Carlo (PIMC) is presented for a realistic plasma model. An intuitive picture emerges.

The usual formula for nuclear reaction rates,  $R$ , per volume, depends on the density of target nuclei, a nuclear cross section  $\sigma$  and the flux of incident particles averaged over a Maxwellian velocity distribution [1]. Density effects on  $R$  are included by multiplying by  $g(0)/g_{bin}(0)$ , the ratio of the actual to the isolated pair limit of the pair distribution function at contact.

The pair distribution function,  $g(r)$ , (species subscripts required in general are omitted for simplicity) is defined by

$$n g(r) = \left\langle \frac{1}{N} \sum_{i \neq j} \delta(r - r_{ij}) \right\rangle \equiv n g_{bin}(r) e^{H(r)}. \quad (1)$$

$g_{bin}(r)$  is the the pair distribution for a two particle system. For a classical Coulomb system  $g_{bin}(r) = \exp(-\beta Z^2/r)$ . For the quantum case the necessary solution to the two body problem to obtain  $g_{bin}(r)$  can be done by routine numerical or analytic methods [2].

The term of interest,  $H(r)$  defined here, represents many body effects. Intuitively  $H(r)$  describes the *crowding* effect due to the interactions of the surrounding particles with the reacting pair which produces an increase in  $g(0)$  over the low density limit.  $H(0)$  is referred to as the *enhancement* factor.

Changes in the system Hamiltonian or its treatment in a calculation will affect both  $g_{bin}(r)$  and  $H(r)$ , usually in opposite ways. For example as shown by Gamow [3] and

others [4] a quantum treatment of the repulsive Coulomb interaction produces a nonzero overlap probability or  $g_{bin}(0)$ . The effect on  $H(0)$  however, is to reduce it from its value for a classical system. Similarly a change in the pair interaction reflecting increased electron screening also increases  $g_{bin}(0)$  while decreasing  $H(0)$ .

The importance of these many body effects to nuclear reactions in plasma was first studied by Salpeter [5]. DeWitt, Graboske and Cooper [6] later used the Monte Carlo simulations of Brush, Sahlin and Teller [7] to extract  $H(r)$  for a classical system of ions in a uniform electron background, the one component plasma (OCP).

This letter presents a study of quantum effects in the many body enhancement of the contact probability for the OCP. It is found that quantum effects significantly reduce this many body enhancement below that found for the classical system. This quantum reduction has an easy intuitive explanation discussed below. Results from the PIMC computations [8] are compared to a variety of semi-quantitative models. Previous work on this system [9, 10] has suggested that quantum fluctuations, or *quantum mechanical spreading*, in the surrounding particles at low temperatures cause a significant enhancement in  $H(0)$  over the classical value rather than the reduction found here.

The OCP does not include electron screening effects. These effects are considered next using a screened ion-ion potential. Finally the importance of ion exchange on  $H(0)$  is examined using restricted PIMC simulations.

*g(0) for the quantum OCP*– Quantum effects dominate at distances smaller than the deBroglie thermal wavelength,  $\lambda_d^2 \equiv \hbar^2/2\pi m k_B T$ . For Coulomb systems, this *quantum smearing* of the  $1/r$  interaction has two important consequences. Firstly, it produces a nonzero  $g_{bin}(0)$ , or nonzero contact probability, which allows charged particle nuclear reactions to occur. Secondly, if  $\lambda_d$  is comparable to nearest neighbor distances, the effective repulsion between particles is reduced compared to the Coulomb force between classical point charges.

$g_{bin}(r)$ , shown in Fig. 1, illustrates this. The lower

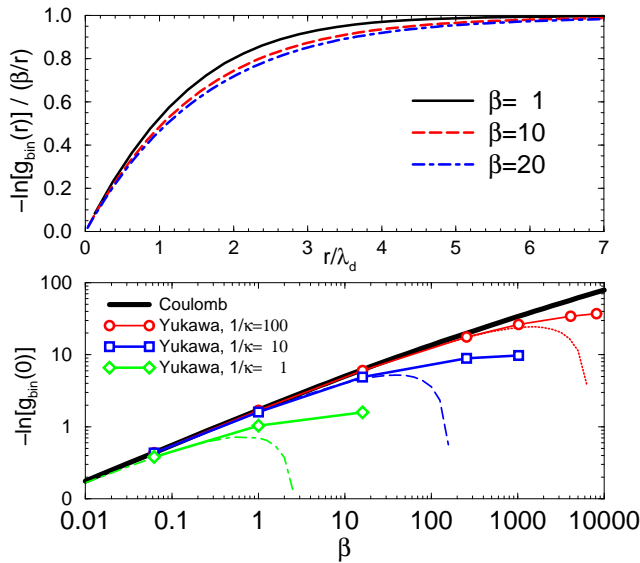


FIG. 1: (color online) Top Panel: Ratio of quantum  $-\ln g_{bin}(r)$  to the classical value,  $\beta/r$ , for various  $\beta$  showing initial reduction followed by convergence to 1 at distances larger than the deBroglie thermal wavelength. Lower panel:  $-\ln g_{bin}(0)$  for protons versus the inverse temperature in ionic atomic units. The solid line is for the Coulomb potential. The solid lines with symbols are for the screened Coulomb potential at indicated screening lengths. Also shown, dotted lines, is the high temperature approximation for the screened Coulomb potential obtained by subtracting  $\beta\kappa$  from the Coulomb result.

panel displays the non-zero  $g_{bin}(0)$ , for both screened and unscreened Coulomb potentials, as a function of inverse temperature. The upper panel shows the reduction in the effective repulsion for  $r < \lambda_d$  for several temperatures. It is this reduction in the effective repulsion between the reacting pair and surrounding particles which reduces  $H(r)$  from its classical value as will be shown below.

The OCP is completely specified by the coupling constant  $\Gamma \equiv \beta Z^2 e^2 / a$ , and a quantum parameter  $\eta \equiv \Gamma / r_s$ , where  $a$  is the ion sphere radius defined by  $n4\pi a^3 / 3 = 1$ , and  $r_s = a / a_{Bohr}$ , the ion sphere radius in terms of the ionic Bohr radius. The quantum parameter is proportional to the squared ratio of the deBroglie thermal wavelength to the ion sphere radius,  $\eta = 2\pi\lambda_d^2 / a^2$ . We also introduce  $h(r)$  defined by  $\Gamma h(r) \equiv H(r)$ . Unless otherwise noted lengths will be ionic Bohr radii,  $a_{Bohr} = \hbar^2 / MZ^2 e^2$ , and energies in ionic Hartrees,  $Z^2 e^2 / a_{Bohr}$ .

The isolated pair radial distribution term is given by the relative Coulomb pair density matrix,  $\rho(r, r'; \beta)$ , at contact [2]

$$g_{bin}(0) = \frac{V\rho(0, 0; \beta)}{\int \rho(r, r; \beta) dr^3} = \frac{\rho(0, 0; \beta)}{\rho_{free}(0, 0; \beta)} \quad (2)$$

$$= (4\pi\beta)^{3/2} \frac{Z^3}{2\pi} \int_0^\infty \frac{k e^{-\beta Z^2 k^2}}{e^{\pi/k} - 1} dk$$

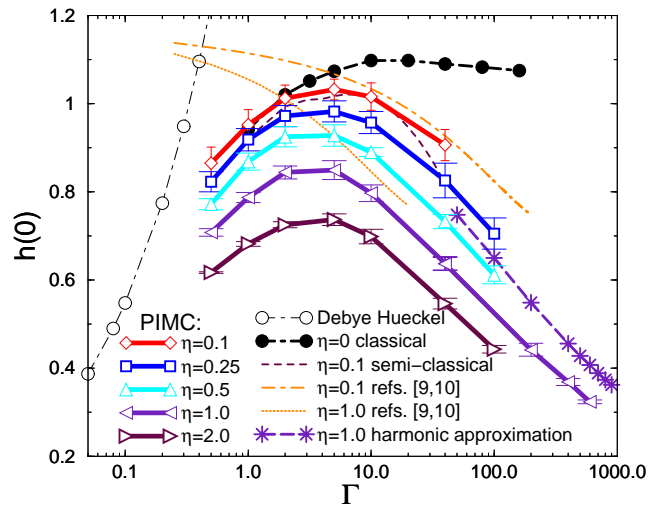


FIG. 2: (color online) Many body enhancement factor,  $h(0) \equiv H(0)/\Gamma$  as a function of the coupling constant,  $\Gamma$ , for various quantum parameters,  $\eta$ . Also shown is the weak coupling, classical Debye-Huckel (DH) limit, a semi-classical approximation, the harmonic approximation (or cell model) and a previous estimate [9, 10].

Unlike the classical case where  $g_{bin}(r) = \exp(-\beta/r)$  is zero at small  $r$ , making it difficult to extract  $h(0)$  from simulation results, the quantum  $g_{bin}(r)$  is finite at the origin. Consequently, the analysis of the simulation results is relatively much easier. For  $\eta > 0.1$ , the computed  $H(r)$  extrapolates without difficulty to  $H(0)$ .

Figure 2 shows the primary results of the PIMC simulations: the many body enhancement factor,  $h(0)$ , as a function of coupling constant  $\Gamma$  for  $\eta = 0.10, 0.25, 0.50, 1.0$ , and  $2.0$ . The values for the classical system are taken from [11–13]. A clear reduction in  $h(0)$  from the classical value is seen which becomes more important at large  $\eta$  or  $\Gamma$ . The trend at large  $\Gamma$  yields reaction rates orders of magnitude lower than would be predicted by classical models. Comparisons with several limits and models, discussed below, are also shown. From Fig. 2 it is seen that the total  $g(0)$  increases with density. The increase in  $g(0)$  with temperature is a balance between two terms: the increase in  $g_{bin}(0)$  with temperature dominating the decrease in the many body term,  $H(0)$ .

As already suggested, a qualitative understanding of the quantum effects on  $h(0)$  can be based on Fig. 1.  $-\ln g_{bin}(r)$  may be viewed as proportional to an “effective” pair potential. Increasing  $\eta$  means that more near neighbors, located roughly one ion sphere radius from the fusing pair, are within a deBroglie thermal wavelength. The “repulsion” between these near neighbors and the fusing pair is thus weaker than in a classical system. This reduced repulsion makes the many body enhancement less important than for the classical system.

For the classical system,  $h(0)$  is related to the nonideal free energy difference between the original plasma and one with two of the ions fused into a doubly charged ion [6, 14],

$$H(r) = -\beta [F(1, N-2) - F(0, N)] - \frac{\Gamma}{4}(r/a)^2 + O(r^4). \quad (3)$$

The arguments in  $F$  represent the number of doubly and singly charged ions. Using the Debye-Huckel free energies [15] for the two cases gives the weak coupling limit,  $h(0) = \sqrt{3\Gamma}$ , shown in Fig. 2. The classical values will approach this for  $\Gamma \leq 0.1$ .

For the quantum case, this free energy relation no longer holds [16]. However to lowest order in  $\eta$  and  $r$  [17]

$$H(r) = -\beta [F(1, N-2) - F(0, N)] - \frac{\Gamma}{4a^2} \langle r^2 \rangle \quad (4)$$

where  $H(r)$  is defined based on the quantum mechanical  $g_{bin}(r)$ , the  $F$ s are the fully quantum mechanical free energies and  $\langle r^2 \rangle$  can be calculated from the relative part of the pair density matrix,

$$\langle r^2 \rangle(r, \beta) \equiv \frac{1}{\beta} \int_0^\beta ds \int d\mathbf{r}' \frac{\rho(\mathbf{r}, \mathbf{r}'; \beta - s) r'^2 \rho(\mathbf{r}', \mathbf{r}; s)}{\rho(\mathbf{r}, \mathbf{r}; \beta)}. \quad (5)$$

In the classical limit  $\langle r^2 \rangle = r^2$ , reproducing Eq. 3. In general

$$\langle r^2 \rangle(r, \beta) = r^2 + \alpha(r, \beta) \frac{\hbar^2 \beta}{m} \quad (6)$$

where the defined function  $\alpha(r, \beta)$ , multiplying the free particle result, tends to 1 as  $\beta \rightarrow 0$ . The second term in Eq. 6, and higher order corrections to Eq. 4, do not vanish as  $r \rightarrow 0$ . Therefore the quantum  $H(0)$  is not obtainable simply from the the first term in Eq. 4, the free energy differences.

Using Eq. 6 together with the first order Wigner-Kirkwood quantum correction for the free energy [18], Eq. 4 gives the lowest order quantum correction to the enhancement factor

$$h(0)[\Gamma, \eta] - h(0)[\Gamma, 0] \approx -\frac{\eta}{4} [\alpha(0, \Gamma^2/\eta) - 1/2]. \quad (7)$$

The spatial integral for  $\alpha(0, \beta)$  reduces to a radial integration. The result is shown for  $\eta = 0.1$  on Fig. 2 and qualitatively reproduces the PIMC results showing significant reduction from the classical  $h(0)$ .

At large  $\Gamma$ , ( $\Gamma \approx 170$  for the classical case), the OCP solidifies into a BCC lattice which can be described in the harmonic approximation. This approximation reproduces the the velocity autocorrelation function, even in the fluid phase, and  $g(r)$  in the solid for  $r$  slightly inside the first peak and beyond [19]. However since  $g(r)$  in the harmonic approximation is given by Gaussians centered on the neighboring atoms with a variance depending by

the curvature of the local potential it erroneously predicts  $g(0) \neq 0$  for the classical case and is of little use in predicting  $H(r)$  at small  $r$  for  $\eta = 0$ .

Explicitly the pair distribution function in the harmonic approximation is [20]

$$ng(\mathbf{r}) = \frac{1}{N} \sum_i \sum_j \frac{\exp[-(\mathbf{r} - \mathbf{R}_{ij}) \cdot \mathbf{M}^{-1} \cdot (\mathbf{r} - \mathbf{R}_{ij})/2]}{\sqrt{(2\pi)^3 |\mathbf{M}|}} \quad (8)$$

where  $\mathbf{M}$  is the pair displacement correlation matrix calculable from the eigenvectors and eigenfrequencies of the dynamical matrix and the  $\mathbf{R}_i$  are lattice sites.

Although always an over estimate, the harmonic approximation result for  $h(0)$  at large  $\eta$  and  $\Gamma$ , where it should be most reliable, reproduces the trends and asymptotic behavior shown by the PIMC results as seen in Fig. 2.

Also shown in Fig. 2 is a fit from an earlier PIMC study [10]

$$h(0) = 1.132 - .0094 \ln \Gamma - (5/32)\xi^2 \quad (9)$$

$$(1 - .0348\xi - .1388\xi^2 + .0222\xi^3) + .0015\xi^3$$

where  $\xi^{3/2} = \frac{2}{\pi} \sqrt{\eta \Gamma}$ . Although the first two terms in this fit, representing the classical  $h(0)$ , have the wrong functional form at low  $\Gamma$ , the succeeding quantum corrections are in agreement with the present PIMC results. This is at variance with the suggestion in [9] that there is an enhancement associated with magnified, coherent quantum fluctuations of the surrounding particles near the pair undergoing fusion.

*Screened Coulomb Potentials*– The OCP model discussed above ignores electron screening. We consider the Yukawa potential

$$V(r) = \frac{e^{-\kappa r}}{r} \quad (10)$$

as an example of an effective electron screened ion-ion potential. In applications the inverse screening length  $\kappa$  may be approximated from the plasma dielectric function [21]

$$\kappa = \lim_{r \rightarrow 0} \left( \frac{1}{r} - \frac{e^{-\kappa r}}{r} \right) \approx \sum_{\mathbf{k}} \frac{4\pi}{\Omega k^2} \left[ 1 - \frac{1}{\epsilon(k)} \right]. \quad (11)$$

These effective ion potential simulations could be supplemented by PIMC computations on hydrogen, explicitly including electrons at low values of  $\eta$  [22].

$g_{bin}(0)$  is shown for this potential for several  $\kappa$  values in the lower panel of Fig. 1. At high temperature, where the thermal deBroglie wavelength is much less than the screening length  $1/\kappa$ , the potential difference  $(e^{-\kappa r} - 1)/r$  may be approximated as constant so  $g_{bin}^{Screened}(0) \approx \exp(\beta \kappa) g_{bin}^{Coul}(0)$ . This constant potential difference approximation is valid and widely used in most astrophysical applications [1] but, as seen in Fig. 1

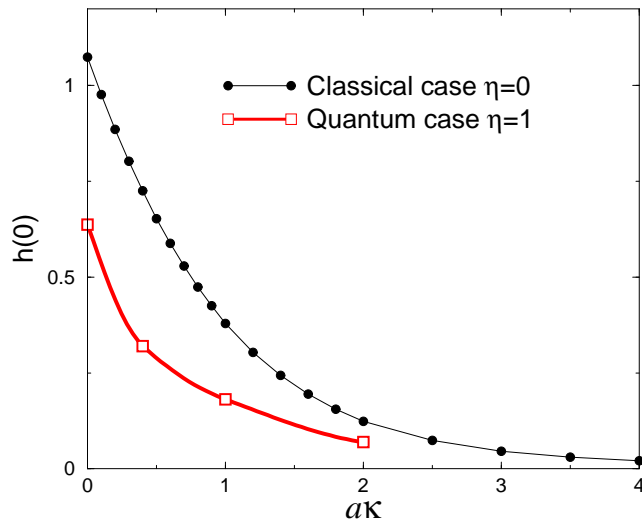


FIG. 3: (color online)  $h(0)$  for the classical [23],  $\eta = 0$ , and quantum,  $\eta = 1$ , Yukawa system at  $\Gamma = 40$  as a function of the inverse screening length  $\kappa$  times ion sphere radius  $a$ .  $\kappa = 0$  corresponds to the unscreened Coulomb potential results in Fig. 2.

(lower panel, dotted lines), it can dramatically overestimate  $g_{bin}(0)$  at low temperatures.

Screening has been shown to reduce  $h(0)$  in the classical OCP [23]. Its effect in the quantum OCP, shown in Fig. 3, is similar. The reduced repulsion from surrounding ions due to screening again reduces the enhancement effect.

*Exchange effects*— Since the quantum parameter  $\eta$  is related to the ratio of deBroglie thermal wavelength to the ion sphere radius it is expected that ion exchange effects could become important under extreme conditions when  $\eta \geq 1$ .

The restricted PIMC simulation technique is used to deal with the fermion sign problem [24]. Free particle nodes are used to restrict the paths. Unlike the preceding computations, restricted PIMC is approximate but is expected to be highly accurate for this system [25].

Due to the Pauli principle the contact probability is zero for particles with the same spin. This effectively increases the ion repulsion and would be expected to increase  $h(0)$ . The results in Fig. 4 show, however, only a slight enhancement over a wide range of the quantum parameter  $\eta$  and confirm that ion exchange effects are unimportant for  $\eta < 1$ .

In conclusion, quantum effects have been shown to significantly reduce the many body enhancement factor which determines nuclear reaction rates in dense plasmas. Electron screening effects produce a further reduction while ion exchange effects are minor.

We thank Berni Alder, Randy Hood, Jeff McAninch and Steve Libby for useful discussions. We particularly thank H. DeWitt for numerous conversations and for

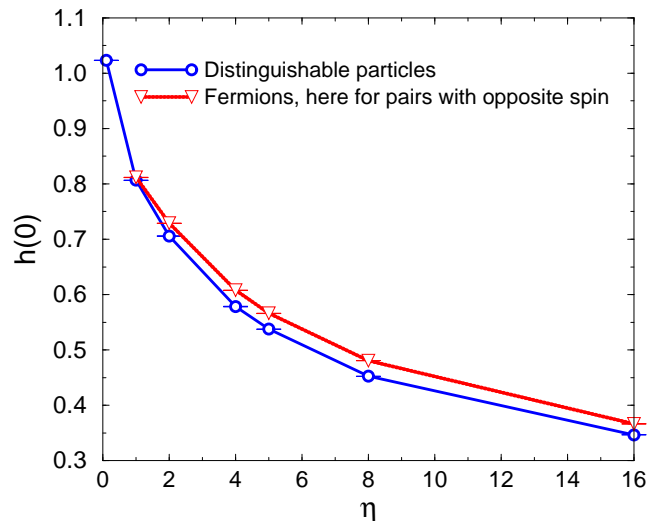


FIG. 4: (color online) Effect of ionic exchanges in the quantum OCP on the enhancement factor,  $h(0)$  at  $\Gamma = 10$  for opposite spin particles. The system contained an equal mixture of spin up and spin down particles.

sharing his unpublished results for several of the classical  $h(0)$  values displayed in figure 2. This work was performed under the auspices of the U.S. Department of Energy by University of California Lawrence Livermore National Laboratory under contract No. W-7405-Eng-48.

- 
- [1] Donald D. Clayton, *Principles of Stellar Evolution and Nucleosynthesis*, Univ. of Chicago Press (1983).
  - [2] E. L. Pollock, *Comp. Phys. Comm.* **52**, 49 (1988).
  - [3] G. Gamow, *Z. Phys.* **51**, 204 (1928).
  - [4] Eugene Merzbacher, *Physics Today* 44 (Aug. 2002).
  - [5] E. E. Salpeter, *Australian J. Phys.* **7**, 373 (1954). E. E. Salpeter and H. M. Van Horn, *Astrophysical J.* **154**, 183 (1969).
  - [6] H. E. Dewitt, H. C. Graboske and M. S. Cooper, *Astrophysical J.* **181** 439 (1973).
  - [7] S. G. Brush, H. Sahlin and E. Teller, *J. Chem. Phys.* **45** 2102 (1966).
  - [8] A product of exact pair density matrices is used for the high temperature density matrix in the PIMC simulations on periodic systems of 54 and 128 particles. Path discretizations between 10 and 400 gave more than adequate convergence.
  - [9] S. Ogata, *Phys. Rev. Lett.* **77** 2726 (1996).
  - [10] S. Ogata, *Astrophysical J.* **481** 883 (1997).
  - [11] H. E. Dewitt and W. Slattery, *Contrib. in Plasma Phys.* **39**, 133 (1999).
  - [12] J.-M. Cailloil and D. Gilles, *Contrib. Plasma Phys.* **39**, 97 (1999).
  - [13] S. Ogata *Phys. Rev. E* **53**, 1094 (1996).
  - [14] B. Jancovici, *Jour. of Stat. Phys.* **17**, 357 (1977).
  - [15] L. D. Landau and E. M. Lifshitz, *Statistical Physics*, Pergamon Press (1969) Section 75.
  - [16] A. Alastuey and B. Jancovici, *Ap. J.* **226**, 1034 (1978).
  - [17] E.L. Pollock and Burkhard Militzer, in preparation.

- [18] L. D. Landau and E. M. Lifshitz, *op. cit.* sect. 33.
- [19] D. A. Baiko, D. G. Yakovlev, H. E. Dewitt and W. L. Slattery, *Phys. Rev. E* **61**, 1912 (2000).
- [20] Alfred A. Kugler, *Annals of Physics* **53**, 133 (1969). A table of eigenfrequencies and eigenvectors for the Wigner lattice is included here.
- [21] J. M. Ziman, *Principles of the Theory of Solids*, Cambridge Press (1965). Eqn. 5.18
- [22] B. Militzer and D. M. Ceperley, *Phys. Rev. Lett.* **85**, 1890 (2000).
- [23] J.-M. Caillol and D. Gilles, *J. Phys. A: Math. Gen.* **36** 6243 (2003)
- [24] D. M. Ceperley, *J. Stat. Phys.* **63**, 1237 (1991).
- [25] M.D. Jones and D. M. Ceperley, *Phys. Rev. Lett.* **76**, 4572 (1996).